Biochemical and Biophysical Research Communications 389 (2009) 57–62

Contents lists available at ScienceDirect

Biochemical and Biophysical Research Communications

journal homepage: www.elsevier.com/locate/ybbrc

A novel fibronectin type III module binding motif identified on C-terminus of *Leptospira* immunoglobulin-like protein, LigB

Yi-Pin Lin [a], Alex Greenwood [c], WeiWei Yan [a], Linda K. Nicholson [c], Yogendra Sharma [d], Sean P. McDonough [b], Yung-Fu Chang [a,*]

[a] Department of Population Medicine and Diagnostic Sciences, College of Veterinary Medicine, Cornell University, Ithaca, NY 14853, USA
[b] Department of Biomedical Sciences, College of Veterinary Medicine, Cornell University, Ithaca, NY 14853, USA
[c] Department of Molecular Biology and Genetics, College of Agriculture and Life Science, Cornell University, Ithaca, NY 14853, USA
[d] Center for Cellular and Molecular Biology, Uppal Road, Hyderabad 500 007, India

ARTICLE INFO

Article history:
Received 31 July 2009
Available online 21 August 2009

Keywords:
Leptospira interrogans
Fibronectin
Type III modules
LigB

ABSTRACT

Infection by pathogenic strains of *Leptospira* hinges on the pathogen's ability to adhere to host cells via extracellular matrix such as fibronectin (Fn). Previously, the immunoglobulin-like domains of *Leptospira* Lig proteins were recognized as adhesins binding to N-terminal domain (NTD) and gelatin binding domain (GBD) of Fn. In this study, we identified another Fn-binding motif on the C-terminus of the *Leptospira* adhesin LigB (LigBCtv), residues 1708–1712 containing sequence LIPAD with a β-strand and nascent helical structure. This motif binds to 15th type III modules ($15F_3$) (K_D = 10.70 μM), and association (k_{on} = 600 M^{-1} s^{-1}) and dissociation (k_{off} = 0.0129 s^{-1}) rate constants represents a slow binding kinetics in this interaction. Moreover, pretreatment of MDCK cells with $LigB_{1706–1716}$ blocked the binding of *Leptospira* by 39%, demonstrating a significant role of $LigB_{1706–1716}$ in cellular adhesion. These data indicate that the LIPAD residues ($LigB_{1708–1712}$) of the *Leptospira interrogans* LigB protein bind $15F_3$ of Fn at a novel binding site, and this interaction contributes to adhesion to host cells.

Introduction

Leptospirosis, caused by infection with pathogenic spirochete *Leptospira* spp., is a serious zoonosis with world-wide distribution [1]. These spirochetes usually penetrate through mucosal surfaces and/or skin wounds and disseminate to several organs, especially the kidney, liver, and lungs. Infection may lead to Weil's disease, which results in liver failure (jaundice), renal failure (nephritis), pulmonary hemorrhage and/or meningitis [1]. Human leptospirosis is often waterborne, and most commonly occurs in tropical areas of the world [1] and remerging in the United States [2].

Many microbial pathogens produce Microbial Surface Components Recognizing Adhesive Matrix Molecules (MSCRAMM) to facilitate their colonization of host tissues during initial infection [3]. Pathogenic leptospires bind to mammalian cells, such as MDCK cells often via the extracellular matrix (ECM) and several adhesion molecules have been identified from *Leptospira* spp. [4–6].

Leptospiral immunoglobulin-like proteins, LigA and LigB, possess 12 and 13 immunoglobulin-like (Ig-like) domains are recognized as MSCRAMMs [7,8]. The binding of LigB to Fn is also modulated by calcium [9]. These studies indicate that Lig proteins are pivotal virulence factors of pathogenic *Leptospira* spp.

In previous studies, strong and mild affinity Fn-binding sites were located on LigB within Ig-like domains of LigB (LigBCen) and the C-terminal variable (LigBCtv) regions, respectively (Fig. 1A) [4,5]. Here, we have further localized the Fn-binding motif of LigBCtv to amino acids (AA) 1708–1712, this sequence binds to the $15F_3$. This significant inhibition of cell binding by this short peptide demonstrates the importance of this sequence in adhesion of the pathogen to target tissues.

Materials and methods

Bacterial strains and cell culture. Leptospira interrogans serovar Pomona (NVSL1427-35-093002) was used as previously described [10]. Leptospires were grown in EMJH medium at 30 °C for less than five passages; growth was monitored by dark-field microscopy [10]. Madin–Darby canine kidney (MDCK) cells (ATCC CCL34™) were cultured in Dulbecco's minimum essential medium (DMEM) containing 10% fetal bovine serum (GIBCO Laboratories, Grand Island, NY). Cells were grown at 37 °C in a humidified atmosphere with 5% CO_2.

Reagents and antibodies. Horseradish peroxidase (HRP)-conjugated streptavidin or goat anti-hamster antibody was purchased from Zymed (San Diego, CA) or Biosource (Camarillo, CA), respectively. FITC-conjugated streptavidin was purchased from Molecular

* Corresponding author. Fax: +1 607 253 3943.
E-mail address: yc42@cornell.edu (Y.-F. Chang).

0006-291X/$ - see front matter © 2009 Elsevier Inc. All rights reserved.
doi:10.1016/j.bbrc.2009.08.089

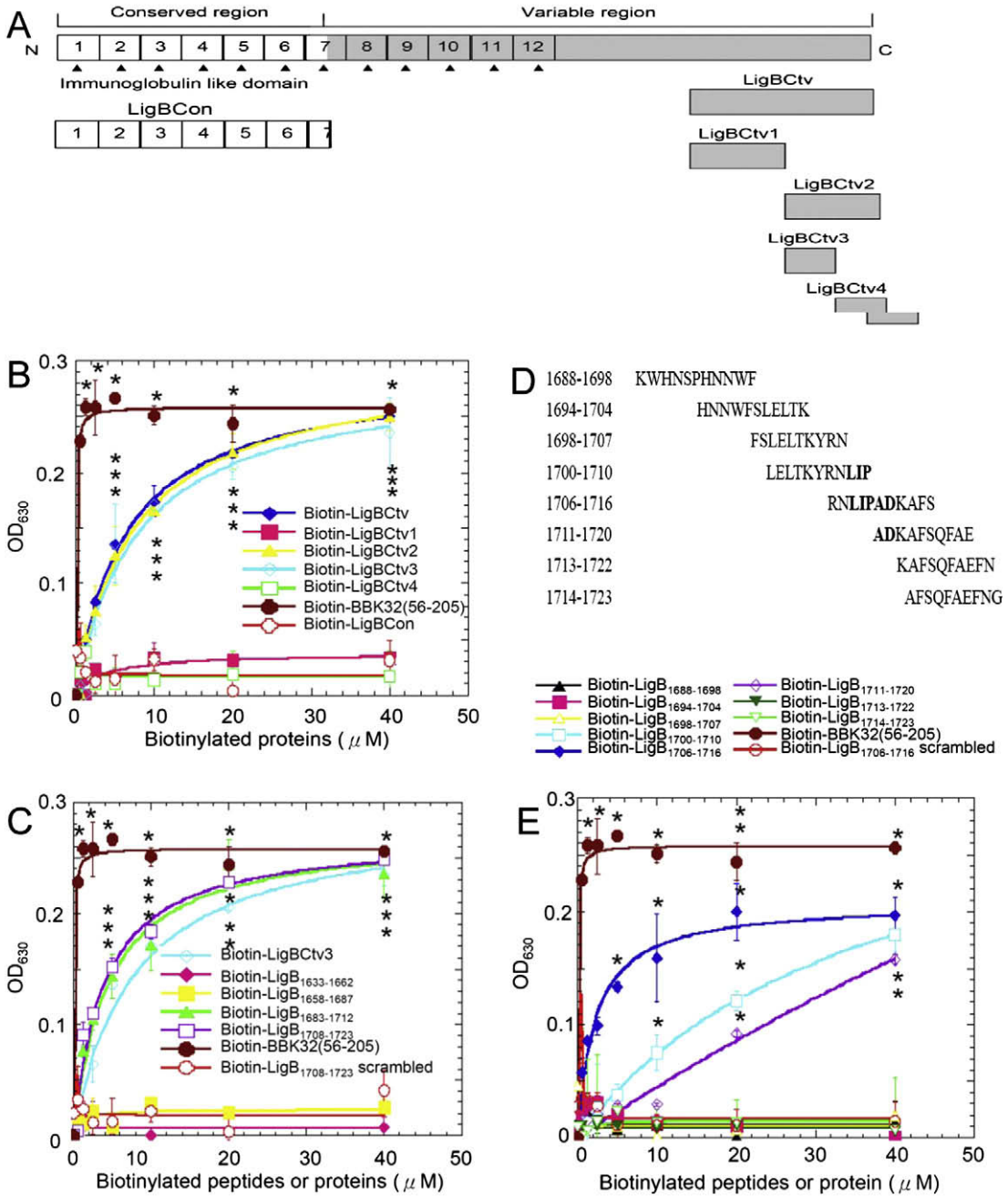

Fig. 1. Identification of Fn-binding residues on LigBCtv. (A) A schematic diagram showing the truncated LigBCtv used in this study. (B) The Fn-binding activity of LigBCtv1, LigBCtv2, LigBCtv3, and LigBCtv4 regions. (C) The Fn-binding activity of the 30mers peptides from LigBCtv. (D) The synthetic peptide sequences (11mers) with overlapping regions used to identify the essential amino acids (indicated in bold) required for Fn binding. (E) The synthetic peptides indicated in (D) used in the Fn-binding assays. Various concentrations (40, 20, 10, 5, 2.5, 1.25, and 0.625 μM) of each tested biotinylated-protein or -peptide, -BBK32$_{56-205}$ (positive control; B, C, and E), -LigBCon (negative control; B) or -scrambled peptide (negative control; C and E) were used in this study. Bound proteins or peptides were measured by ELISA.

Probes (Eugene, OR). Cell binding domain (CBD, 120 kDa) or 40 kDa domain (40 kDa) of Fn were purchased from Chemicon International (Temecula, CA). Anti-*L. interrogans* antibodies were previously prepared in hamsters from the challenge controls [10]. Full length human plasma Fn, N-terminal domain (NTD) or gelatin binding domain (GBD) of Fn were purchased from Sigma (St. Louis, MO), and Biotin labeling kit were purchased from Pierce (Rockford, IL).

Plasmid construction and protein purification. Rat 12th–13th, 14th, or 15th type III modules were purified as maltose binding protein (MBP) fusion proteins (Fig. 3A) [11]. The DNA fragments of LigBCon and BBK32 (AA 56–205) were inserted into pGEX-4T-2 (GE, Piscataway, NJ) [10]. LigBCtv was analyzed with Jpred to predict the secondary structure for truncation construction. Constructs for the expression of GST fused with LigBCtv1 (AA 1418–1632), LigBCtv2 (AA 1633–1889), LigBCtv3 (AA 1633–1723) and LigBCtv4 (AA 1724–1889) were generated using the vector pGEX-4T-2 (Fig. 1A). Relevant fragments of DNA were amplified by PCR using primers (Supplemental Table 1) based on the *ligB* sequence [7]. Primers were engineered to introduce a BamHI or SalIsite at the 5′ end of each fragment and a stop codon followed by a SalI or NotI site at the 3′ end of each fragment. PCR products were digested sequentially with BamHI/SalI or SalI/NotI for the indicated fragment and then ligated into pGEX-4T-2. In this study, we purified the soluble form of the four GST fusion peptides from *Escherichia coli* as previously described [7].

Binding assays by ELISA. To determine the binding of truncated LigB (LigBCtv1, LigBCtv2, LigBCtv3, or LigBCtv4) or LigB peptides to Fn, 1 μg of Fn or BSA (negative control) was coated onto microtiter plate wells described previously [4,5]. Then, various concentrations (as indicated in Figs. 1 and 3) of biotinylated LigB truncated protein, LigB peptide (Figs. 1B, C, and E and 3), scrambled peptide (negative control, Supplemental Table 2), BBK32 (56–205) (positive control, [12] or LigBCon (negative control, [5]) was added to each microtiter plate wells for 1 h at 37 °C. To measure the binding of biotinylated LigB protein, HRP-conjugated streptavidin was added into microtiter plate wells (1:1000).

To identify the binding site of $LigB_{1706–1716}$ on Fn, 1 μg of each full length Fn, NTD, GBD, CBD, 40 kDa domain of Fn, or MBP fused with 12th–13th type III modules (MBP-12–$13F_3$), 14th type III modules (MBP-$14F_3$), or 15th type III modules (MBP-$15F_3$) of Fn and MBP (negative control) were coated onto microtiter plate wells. Then, various concentrations (as indicated in Fig. 3B and C) of biotin-conjugated $LigB_{1706–1716}$ (biotin-$LigB_{1706–1716}$) or biotin (negative control, data not shown) were added to microtiter plate wells. To measure the binding of $LigB_{1706–1716}$ to MDCK cells, MDCK cells (10^5) were incubated with various concentrations (as indicated in Fig. 4A) of biotin-$LigB_{1706–1716}$ or biotin (negative control) in 100 μl PBS for 1 h at 37 °C. To measure the binding inhibition of *Leptospira* to MDCK cells treated with $LigB_{1706–1716}$, MDCK cells (10^5) were pretreated with various concentrations (as indicated in Fig. 4B) of biotin-$LigB_{1706–1716}$ or biotin (negative control) in 100 μl PBS for 1 h at 37 °C. Then, the following steps such as the addition of *Leptospira*, plate washing, and the incubation and usage of antibodies were described previously [5]. To detect the binding of biotin-$LigB_{1706–1716}$ or biotin to Fn or MDCK cells, HRP-conjugated streptavidin (1:1000) was added and incubated for 30 min at 25 °C. The measurement of the binding by ELISA was described previously [5].

NMR sample preparation and experiments. 2.51 mM of cysteine conjugated $LigB_{1703–1717}$ in PBS (pH 6.0) in either H_2O or D_2O was applied to NMR. NMR spectra were recorded at 25 °C on a Varian Inova 600 MHz spectrometer using the States-Haberkorn hypercomplex method of frequency discrimination [12]. Two-dimensional homonuclear total correlation spectroscopy (TOCSY) [13] and nuclear Overhauser enhancement spectroscopy (NOESY) [14] spectra were recorded with spectral widths of 6 kHz in $t1$ (1024 real + imaginary data points in the TOCSY and H_2O NOESY experiments, 800 real + imaginary in the D_2O NOESY experiment) and 8 kHz in $t2$ (2048 real + imaginary data points). Two-dimensional TOCSY spectra were acquired with a DIPSI-2 [15] isotropic mixing period (t_{mix}) of 55 ms, and NOESY spectra were acquired with a t_{mix} of 200 ms. For both experiments, the spectra were processed to a final data size of 1024 by 2048 real points.

NMR data were processed and analyzed using the software tools nmrPipe and nmrDraw [16]. Solvent subtraction was obtained by subtraction of a fourth-order polynomial fit in the time domain. The free induction decay (FID) was generally multiplied by a 72^o shifted squared sine-bell function before zero-fitting and Fourier transformation. Linear baseline correction was applied in the acquisition dimension of all spectra. Analysis of the resulting TOCSY and NOESY spectra yielded proton resonance assignments for all 16 LigB-derived residues (Supplemental Table 3). Cys1 and Thr2 lack δ_{HN} assignments because of fast proton exchange of the N-terminal amino group.

Fluorescence spectrometry. Intrinsic fluorescence emission spectra were measured on a Hitachi F4500 spectrofluorometer (Hitachi, San Jose, CA). All conditions of recorded spectra were described previously [6]. For $LigB_{1706–1716}$ titration, various concentrations of $LigB_{1706–1716}$ (as indicated in Fig. 3D) was mixed with 1 μM of $15F_3$ of Fn and spectra were recorded after 5 min. To determine the dissociation constant (K_D), the fluorescence intensities at 350 nm were recorded and fitted by using KaleidaGraph software (Version 2.1.3 Abelbeck software). All of the measurements were corrected for dilution and for inner filter effect.

Stopped-flow measurements. Stopped-flow measurements were performed using a KinTek stopped flow system (Austin, TX). Trp fluorescence emission above 320 nm was monitored using an excitation wavelength of 295 nm and a 320 nm cut-off filter at 25 °C. The stopped-flow experiments were performed by mixing Fn $15F_3$ in PBS after mixing with increased concentrations of $LigB_{1706–1716}$; the time course of fluorescence intensity change was recorded by 1000 pairs of data in each experiment, and sets of data from three experiments were averaged. The apparent observed rate (k_{obs}) was obtained by fitting the stopped-flow trace (average of five repeated runs) with a single exponential equation as shown follows.

$$F_t = A\exp(-k_{obs}t) + F_\infty \quad (1)$$

where F_t is the fluorescence observed at any time, t, and A is the signal amplitude. F_∞ is the final value of fluorescence, and k_{obs} is the observed first order rate constant. The residuals were measured by the differences between the calculated fit and the exponential data. To calculate k_{on} and k_{off} of the binding reaction, the concentrations of $LigB_{1706–1716}$ were at least 25-fold higher than that of $15F_3$ to fulfill the requirement of pseudo-first order so k_{obs} obtained from different concentrations of $LigB_{1706–1716}$ could fit the following equation to determine the value of k_{on} and k_{off}.

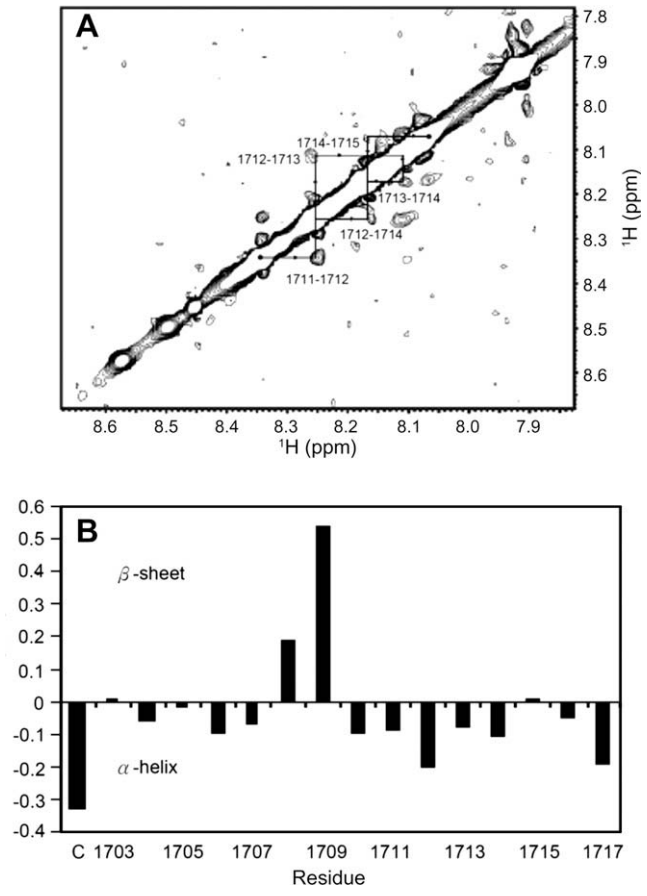

Fig. 2. (A) H^N–H^N region of the homonuclear NOESY spectrum (t_{mix} = 200 ms, pH 6.0) of $LigB_{1703–1717}$ in PBS in H_2O. The d_{NN} cross-peaks are labeled with residue numbers, and arrows indicate sequential connectivities. The NOEs between sequential residues in residues A_{1711} through F_{1715} indicate nascent helical character. (B) Plot of the difference in H^α chemical shifts, or $\Delta\delta_{H\alpha}$, between observed and random coil values for $LigB_{1703–1717}$. (C) Indicated the first cysteine conjugated on $LigB_{1703–1717}$. A stretch of $\Delta\delta_{H\alpha}$ values below −0.1 indicates nascent α-helical structure, and a stretch of values above 0.1 indicates preference for β-strand conformation.

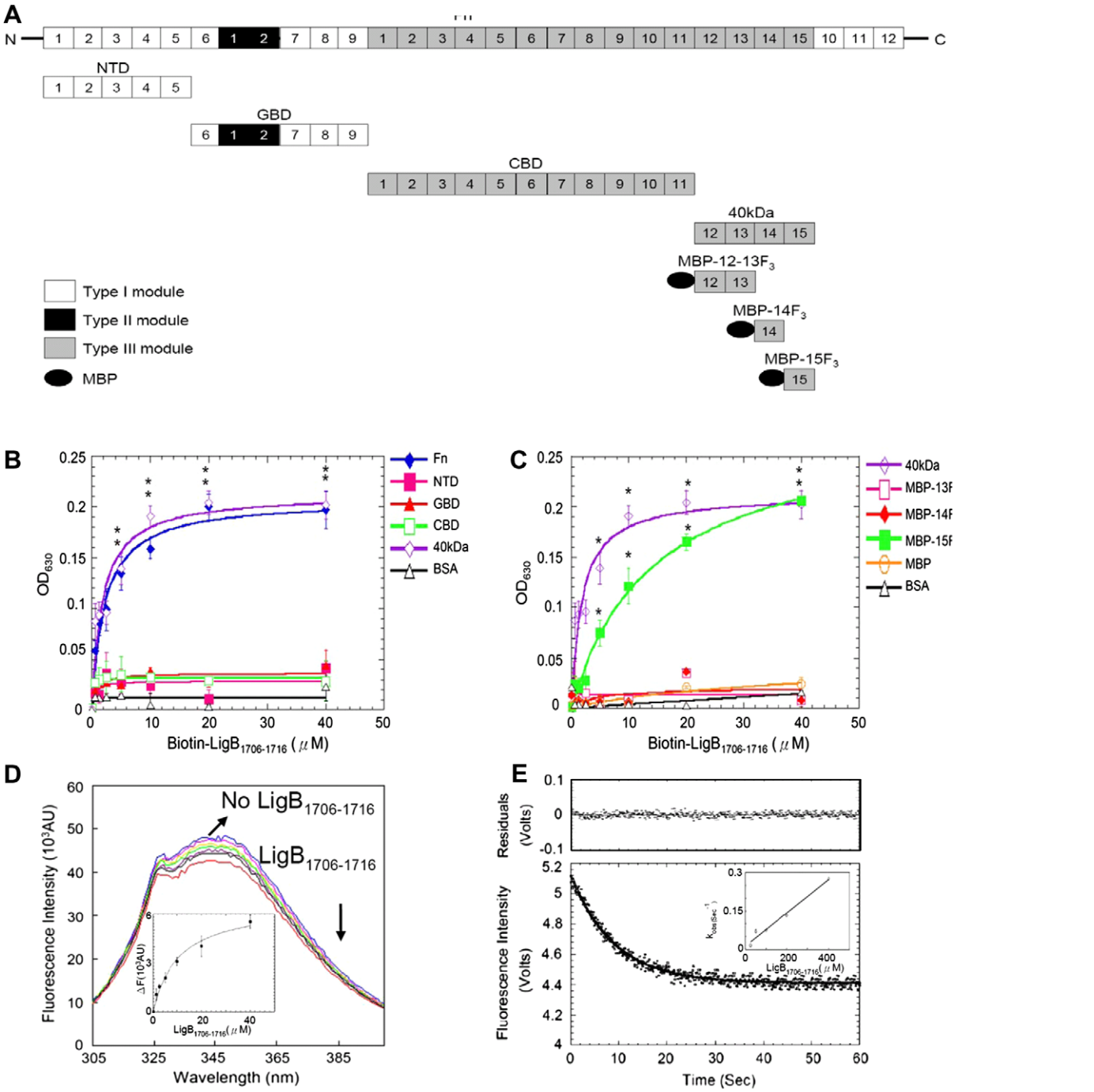

Fig. 3. Mapping and characterization of $LigB_{1706–1716}$ binding sites on Fn. (A) A chart presenting Fn and truncated Fn used in this study. (B,C) Various concentration (0.625, 1.25, 2.5, 5, 10, 20, 40 μM) of biotin-$LigB_{1706–1716}$ or biotin (negative control and data not shown) were added to 1 μg of (B) Fn, NTD, GBD, CBD, 40 kDa, or BSA (negative control) (C) 40 kDa, MBP-12–$13F_3$, MBP-$14F_3$, MBP-$15F_3$, MBP (negative control), or BSA (negative control) coated microtiter plate wells. Bound proteins were measured by ELISA. (D) 1 μM of $15F_3$ in PBS in the presence of 0, 0.625, 1.25, 2.5, 5, 10, 20 and 40 μM of $LigB_{1706–1716}$ was excited at 295 nm to measure Trp fluorescence. Inner plot: K_D of $15F_3$-$LigB_{1706–1716}$ determined by monitoring quenching fluorescence intensities at 350 nm. (E) Stop flow experiment of $15F_3$ binding to $LigB_{1706–1716}$. The signal represents the total fluorescence emission above 320 nm by excited at 295 nm. Inner plot: The kinetic plot of k_{obs} versus concentration of 1 μM $15F_3$ under different $LigB_{1706–1716}$ concentrations (25, 50, 100, 200, 400 μM).

$$k_{obs} = k_{on}[LigB_{1706–1716}] + k_{off} \quad (2)$$

Binding assays by confocal laser-scanning microscopy (CLSM). MDCK cells (10^6) were preincubated with 10 μM of biotin-$LigB_{1706–1716}$ or biotin (negative control) as previously described [5]. Then, 150 μl of FITC-conjugated streptavidin was added (1:250). Fixation and immunofluorescence staining were followed as previously described [5]. Three fields were selected to count the number of binding organisms counted by an investigator blinded to the treatment group. To measure the reduced attachment of *Leptospira*. All studies were repeated three times.

Statistical analysis. Significance between samples was determined using the Student's *t*-test following logarithmic transformation of the data. Two-tailed *P*-values were determined for each sample and a *P*-value < 0.05 was considered significant. Each data point represents the mean ± standard error of the mean (SEM) of

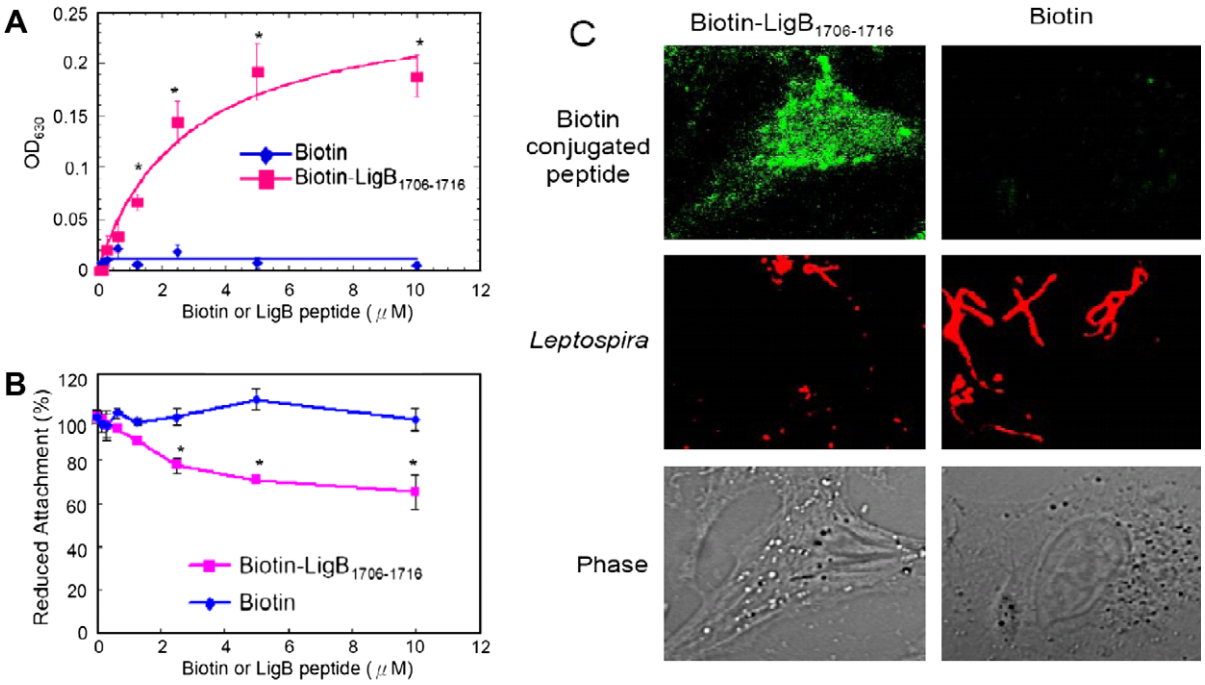

Fig. 4. The binding of $LigB_{1706–1716}$ to MDCK cells reduces leptospiral adhesion. (A) Various concentrations (0, 2, 4, 6, 8, or 10 μM) of biotin-$LigB_{1706–1716}$, or biotin (negative control) were added to MDCK cells (10^5). (B,C) $LigB_{1706–1716}$ inhibits the binding of *Leptospira* to MDCK cells. (B) MDCK cells (10^5) were incubated with various concentrations (0, 2, 4, 6, or 8, 10 μM) of biotin-$LigB_{1706–1716}$, or biotin (negative control) prior to the addition of *Leptospira* (10^7). (A) The binding or (B) the reduced attachment was measured by ELISA. (C) The adhesion of *Leptospira* (10^8) or the binding of 10 μM of biotin or biotin-$LigB_{1706–1716}$ to MDCK cells (10^6) was detected by CLSM.

sample tested in triplicate. An (∗) indicates the result was statistically significant.

Results

LigB residues 1708–1712 (LIPAD) possess Fn-binding activity

To identify the Fn-binding region, truncated LigBCtv including LigBCtv1, LigBCtv2, LigBCtv3, and LigBCtv4 (Fig. 1A) were assayed for Fn-binding capability using ELISA. Only LigBCtv2 and LigBCtv3 bound Fn (Fig. 1B). The Fn-binding region was more finely mapped to LigB residues 1688–1723 using synthesized peptides corresponding to the LigBCtv sequence (Fig. 1C). Then, peptides corresponding to AA 1688–1723 were also synthesized with overlapping regions of five amino acids (Fig. 1D and Supplemental Table 2). Eventually, $LigB_{1706–1716}$ displayed the highest Fn-binding activity, while both $LigB_{1700–1710}$ and $LigB_{1711–1720}$ had moderate Fn-binding affinities (Fig. 1D). Based on the alignment of these three peptides, the residues LIPAD ($LigB_{1708–1712}$) of LigBCtv were found to be essential for Fn binding (Fig. 1E).

β-Strand and nascent helical character are in the peptide containing the LIPAD motif

To reveal the structure of this Fn-binding motif, $LigB_{1703–1717}$, the peptide containing LIPAD residues, was investigated with NMR. As shown in Fig. 2A, nuclear Overhauser effect (NOE) cross-peaks between successive amide protons, or $d_{NN}(i,i+1)$ NOEs, were observed for residues $A_{1711}D_{1712}K_{1713}A_{1714}F_{1715}$ in the NOESY spectra of $LigB_{1703–1717}$. An additional cross-peak between the amide protons of D_{1712} and A_{1714}, or $d_{NN}(i,i+2)$ NOE, was also observed. This pattern of local NOEs is indicative of nascent helical structure, defined as an equilibrium between a series of turn-like structures and unfolded states [17]. Furthermore, the secondary structure of peptides can be elucidated by $\Delta\delta_{H\alpha}$, difference between an observed alpha protons chemical shift and the corresponding random coil value for a given amino acid residue [18]. As shown in Fig. 2B, $\Delta\delta_{H\alpha}$ values greater than +0.1 for sequential residues L_{1708} and I_{1709} (+0.19 and +0.54, respectively), indicating that this segment of the peptide may transiently adopt a β-strand conformation. This region is followed by a nascent helical region for residues $A_{1711}D_{1712}K_{1713}A_{1714}$ consistent with the nascent helical character deduced from the observed NOEs involving these residues as described above. The low value for cysteine, the first amino acid in the peptide (conjugated for mouse immunization) is most likely due to its position near the positive N terminus.

The LigB LIPAD motif binds to the 15th type III module of Fn with slow binding kinetics

ELISA was also performed with biotin-$LigB_{1706–1716}$ and full length or truncated Fn including NTD, GBD, CBD, and 40 kDa to identify the LIPAD-binding site on Fn. The results show that $LigB_{1706–1716}$ binds to Fn and 40 kDa (Fig. 3B). Then, the ELISA applied to biotin-$LigB_{1706–1716}$ with 40 kDa and MBP-12–$13F_3$, MBP-$14F_3$, MBP-$15F_3$ further locate the LIPAD-binding site on $15F_3$ (Fig. 3C) in agreement with the quenching of the intrinsic Trp fluorescence intensity of $15F_3$ in the presence of $LigB_{1706–1716}$ ($K_D = 10.70 \pm 2.23$ μM) (Fig. 3D). The kinetic rates of $LigB_{1706–1716}$–$15F_3$ determined by stop flow experiment ($k_{on} = 600 \pm 12\ M^{-1}\ s^{-1}$ and $k_{off} = 0.0129 \pm 0.0003\ s^{-1}$) are comparatively slow (Fig. 3E). These results indicate that the LIPAD motif binds to the $15F_3$ with a slow binding kinetics.

$LigB_{1708–1712}$ LIPAD residues mediate the attachment of Leptospira to MDCK cells

To investigate the role of the LIPAD residues in cell binding, various concentrations of biotin-conjugated $LigB_{1706–1716}$ or biotin were added to MDCK cells. Our results show that biotin-$LigB_{1706–1716}$ binds to MDCK cells in a dose-dependent manner (Fig. 4A and C). Pretreatment of MDCK cells with biotin-$LigB_{1706–1716}$ re-

duced the attachment of *Leptospira* by approximately 39% compared to either untreated (data not shown) or biotin-treated MDCK cells in a dose-dependent manner (Fig. 4B).

Discussion

Recently, it was shown that the some bacterial Fn-binding proteins binds to NTD by β zipper, two antiparallel β-strands [19], but some binds to the cationic cradle of the $13F_3$ [20]. Here, we show that the LIPAD motif of LigB binds to the $15F_3$, and this motif can also found in other *Leptospira* serovars and zonadhesin, an eukaryotic ECM binding proteins [21]. Our study describes for the first time a bacterial MSCRAMM binding to this module. These results suggest that $LigB_{1706–1716}$ may exploit a novel Fn-binding mechanism.

The immunoglobulin-like repeat regions of LigA and LigB, including LigBCen2, strongly bind to the NTD and GBD [4,5]. This study identifies an Fn-binding LIPAD motif located in the C-terminal non-repeat region of LigB that slowly binds to the $15F_3$ with moderate affinity (K_D = 10.70 μM, k_{on} = 600 M^{-1} s^{-1}, k_{off} = 0.0129 s^{-1}) (Fig. 3). The kinetic rates of $LigB_{1706–1716}$ binding to the $15F_3$ are at least 100-fold slower than rates seen with other bacterial Fn-binding proteins [22]. The slow k_{off} may be an important factor in retention of the bound state in the biological system. In an *in vivo* system where the concentration of ligand is not constant, but rather influenced by factors such as absorption, distribution, metabolism, and excretion (ADME), the residence time of a receptor–ligand complex is not necessarily appropriately described by the equilibrium dissociation constant K_D [23]. Current experimental evidence has pointed to the dissociation rate constant k_{off} as a more relevant parameter in some cases [24]. This has led to arguments that the k_{off} may be an important parameter to consider in drug design and screening. In light of this, it is tempting to interpret the slow k_{off} of the $LigB_{1706–1716}$:Fn complex as an example of an evolutionarily optimized k_{off} for a bacterial adhesin/target complex, which is challenged by many of the same limitations to overall ligand concentration as drug/target complexes are.

It has been indicated a *ligB* mutant with an insertion containing a Spc^r cassette into the 3′ end of the *ligB* gene is still virulent in a hamster model [25]. The reasons are unknown. However, there are several possibilities: (1) LigB is only needed for initial adhesion and invasion of *Leptospira* moving from the environment through mucous membranes and injured skin. (2) The presence of other putative adhesins with potentially redundant functions. To answer these questions, further studies are needed.

We have demonstrated that the sequence LIPAD located on the C-terminus of LigB is an Fn-binding motif that interacts with the 15th type III module of Fn with slow binding kinetics, mediates cell adhesion, and displays β-strand and nascent helix character when free in solution. Work to further elucidate this interaction is in progress in our lab.

Acknowledgments

This work was supported in part by the Biotechnology Research and Development Corporation (BRDC), the Harry M. Zweig Memorial Fund for Equine Research, the National Science Foundation (L.K.N.), an NIH Biophysics Training Grant (A.I.G.), and the New York State Science and Technology Foundation. Thanks to Prof. B.U. Pauli for 12–$13F_3$, $14F_3$, and $15F_3$ clones, Dr. Marci Scidmore for the using of CLFM and to Drs. Jeremiah Hanes's assistance in stopped flow technique.

Appendix A. Supplementary data

Supplementary data associated with this article can be found, in the online version, at doi:10.1016/j.bbrc.2009.08.089.

References

[1] S.B. Faine, B. Adher, C. Bolin, et al., *Leptospira* and Leptospirosis, MedSci, Melbourne, Australia, 1999.
[2] E. Meites, M.T. Jay, S. Deresinski, et al., Reemerging leptospirosis, California, Emerg. Infect. Dis. 10 (2004) 406–412.
[3] U. Schwarz-Linek, M. Hook, J.R. Potts, The molecular basis of fibronectin-mediated bacterial adherence to host cells, Mol. Microbiol. 52 (2004) 631–641.
[4] Y.P. Lin, Y.F. Chang, A domain of the *Leptospira* LigB contributes to high affinity binding of fibronectin, Biochem. Biophys. Res. Commun. 362 (2007) 443–448.
[5] Y.P. Lin, Y.F. Chang, The C-terminal variable domain of LigB from *Leptospira* mediates binding to fibronectin, J. Vet. Sci. 9 (2008) 133–144.
[6] F. Merien, J. Truccolo, G. Baranton, et al., Identification of a 36-kDa fibronectin-binding protein expressed by a virulent variant of *Leptospira interrogans* serovar icterohaemorrhagiae, FEMS Microbiol. Lett. 185 (2000) 17–22.
[7] R.U. Palaniappan, Y.F. Chang, F. Hassan, et al., Expression of leptospiral immunoglobulin-like protein by *Leptospira interrogans* and evaluation of its diagnostic potential in a kinetic ELISA, J. Med. Microbiol. 53 (2004) 975–984.
[8] R.U. Palaniappan, Y.F. Chang, S.S. Jusuf, et al., Cloning and molecular characterization of an immunogenic LigA protein of *Leptospira interrogans*, Infect. Immun. 70 (2002) 5924–5930.
[9] Y.P. Lin, R. Raman, Y. Sharma, et al., Calcium binds to leptospiral immunoglobulin-like protein, LigB and modulates fibronectin binding, J. Biol. Chem. 283 (2008) 25140–25149.
[10] R.U. Palaniappan, S.P. McDonough, T.J. Divers, et al., Immunoprotection of recombinant leptospiral immunoglobulin-like protein A against *Leptospira interrogans* serovar Pomona infection, Infect. Immun. 74 (2006) 1745–1750.
[11] H.C. Cheng, M. Abdel-Ghany, B.U. Pauli, A novel consensus motif in fibronectin mediates dipeptidyl peptidase IV adhesion and metastasis, J. Biol. Chem. 278 (2003) 24600–24607.
[12] D.J. States, R.A. Haberkorn, D.J. Rubena, Two-dimensional nuclear overhauser experiment with pure absorption phase in four quadrants, J. Magn. Reson. 48 (1982) 286–292.
[13] A. Bax, D.G. Davis, MLEV-17 based two-dimensional homonuclear magnetization transfer spectroscopy, J. Magn. Reson. 65 (1985) 355–360.
[14] G. Bodenhausen, H. Kogler, R.R. Ernst, Selection of coherence transfer pathways in NMR pulse experiments, J. Magn. Reson. 58 (1984) 370–388.
[15] A.J. Shaka, C.L. Lee, A. Pines, Iterative schemes for bilinear operators; application to spin decoupling, J. Magn. Reson. 77 (1988) 274–293.
[16] F. Delaglio, S. Grzesiek, G.W. Vuister, et al., NMRPipe: a multidimensional spectral processing system based on UNIX pipes, J. Biomol. NMR 6 (1995) 277–293.
[17] H.J. Dyson, M. Rance, R.A. Houghten, et al., Folding of immunogenic peptide fragments of proteins in water solution. II. The nascent helix, J. Mol. Biol. 201 (1988) 201–217.
[18] D.S. Wishart, B.D. Sykes, F.M. Richards, The chemical shift index: a fast and simple method for the assignment of protein secondary structure through NMR spectroscopy, Biochemistry 31 (1992) 1647–1651.
[19] U. Schwarz-Linek, J.M. Werner, A.R. Pickford, et al., Pathogenic bacteria attach to human fibronectin through a tandem beta-zipper, Nature 423 (2003) 177–181.
[20] R.A. Kingsley, A.M. Keestra, M.R. de Zoete, et al., The ShdA adhesin binds to the cationic cradle of the fibronectin 13FnIII repeat module: evidence for molecular mimicry of heparin binding, Mol. Microbiol. 52 (2004) 345–355.
[21] D.M. Hardy, D.L. Garbers, A sperm membrane protein that binds in a species-specific manner to the egg extracellular matrix is homologous to von Willebrand factor, J. Biol. Chem. 270 (1995) 26025–26028.
[22] B. Kreikemeyer, S. Oehmcke, M. Nakata, et al., *Streptococcus pyogenes* fibronectin-binding protein F2: expression profile, binding characteristics, and impact on eukaryotic cell interactions, J. Biol. Chem. 279 (2004) 15850–15859.
[23] R.A. Copeland, D.L. Pompliano, T.D. Meek, Drug-target residence time and its implications for lead optimization, Nat. Rev. Drug Discov. 5 (2006) 730–739.
[24] A. Berezov, H.T. Zhang, M.I. Greene, Disabling ErbB receptors with rationally designed exocyclic mimetics of antibodies: structure–function analysis, J. Med. Chem. 44 (2001) 2565–2574.
[25] J. Croda, C.P. Figueira, E.A. Wunder Jr., et al., Targeted mutagenesis in pathogenic *Leptospira* species: disruption of the LigB gene does not affect virulence in animal models of leptospirosis, Infect. Immun. 76 (2008) 5826–5833.